6-8-2024

Evaluation of 14 PFAS for permeability and organic anion transporter interactions: Implications for renal clearance in humans

Sangwoo Ryu
University of Rhode Island

Emi Yamaguchi
Pfizer

Seyed Mohamad Sadegh Modaresi
University of Rhode Island

Juliana Agudelo
University of Rhode Island

Chester Costales
Pfizer

See next page for additional authors

Citation/Publisher Attribution

Sangwoo Ryu, Emi Yamaguchi, Seyed Mohamad Sadegh Modaresi, Juliana Agudelo, Chester Costales, Mark A. West, Fabian Fischer, Angela L. Slitt. Evaluation of 14 PFAS for permeability and organic anion transporter interactions: Implications for renal clearance in humans, *Chemosphere*, Volume 361, 2024. https://doi.org/10.1016/j.chemosphere.2024.142390.

Evaluation of 14 PFAS for permeability and organic anion transporter interactions: Implications for renal clearance in humans

Authors

Sangwoo Ryu, Emi Yamaguchi, Seyed Mohamad Sadegh Modaresi, Juliana Agudelo, Chester Costales, Mark A. West, Fabian Fischer, and Angela L. Slitt

Evaluation of 14 PFAS for Permeability and Organic Anion Transporter Interactions: Implications for Renal Clearance in Humans

Sangwoo Ryu[1,2], Emi Yamaguchi[2], Seyed Mohamad Sadegh Modaresi[1], Juliana Agudelo[1], Chester Costales[2], Mark A. West[2], Fabian Fischer[1,3], Angela L. Slitt[1]

[1] Department of Biomedical and Pharmaceutical Sciences, University of Rhode Island, Kingston, RI 02881, United States.

[2] Pharmacokinetics, Dynamics and Metabolism, Pfizer Worldwide Research & Development, Pfizer Inc., Groton, CT 06340, United States.

[3] Harvard John A. Paulson School of Engineering and Applied Sciences, Harvard University, Cambridge, Massachusetts 02138, United States.

Corresponding Authors:

1. Angela L. Slitt, Ph.D.

University of Rhode Island

395D, Avedisian Hall

7 Greenhouse Rd. Kingston

RI 02881, USA

Phone: 401-874-5020

Email: aslitt@uri.edu

2. Fabian C. Fischer, Ph.D.

University of Rhode Island

21 495Q, Avedisian Hall
22 7 Greenhouse Rd. Kingston
23 RI 02881, USA
24 Phone: 401-874-5594
25 Email: fabian.fischer@uri.edu

Abstract

Per- and polyfluoroalkyl substances (PFAS) encompass a diverse group of synthetic fluorinated chemicals known to elicit adverse health effects in animals and humans. However, only a few studies investigated the mechanisms underlying clearance of PFAS. Herein, the relevance of human renal transporters and permeability to clearance and bioaccumulation for 14 PFAS containing three to eleven perfluorinated carbon atoms (η_{pfc} = 3-11) and several functional head-groups was investigated. Apparent permeabilities and interactions with human transporters were measured using *in vitro* cell-based assays, including the MDCK-LE cell line, and HEK293 stable transfected cell lines expressing organic anion transporter (OAT) 1-4 and organic cation transporter (OCT) 2. The results generated align with the Extended Clearance Classification System (ECCS), affirming that permeability, molecular weight, and ionization serve as robust predictors of clearance and renal transporter engagement. Notably, PFAS with low permeability (ECCS 3A and 3B) exhibited substantial substrate activity for OAT1 and OAT3, indicative of active renal secretion. Furthermore, we highlight the potential contribution of OAT4-mediated reabsorption to the renal clearance of PFAS with short η_{pfc}, such as perfluorohexane sulfonate (PFHxS). Our data advance our mechanistic understanding of renal clearance of PFAS in humans, provide useful input parameters for toxicokinetic models, and have broad implications for toxicological evaluation and regulatory considerations.

Keywords: PFAS, renal clearance, ion transporters, permeability

1. Introduction

Per- and polyfluoroalkyl substances (PFAS) are a group of synthetic chemicals with unique heat-resistant and water-repellent properties, which resulted in their extensive use in various commercial and industrial applications. Most PFAS are highly persistent and mobile, resulting in their ubiquitous presence in the environment (Wang et al., 2017) and accumulation in humans (Giesy and Kannan, 2001; Thompson et al., 2011; Wang et al., 2017; Martinez et al., 2022; Nystrom et al., 2022). Human exposure to PFAS has been linked to multiple adverse health effects, including kidney and testicular cancer, decreased vaccine response, reduced birth weight, elevated cholesterol levels, and hypothyroidism (Fei et al., 2007; Barry et al., 2013; Darrow et al., 2013; Geiger et al., 2014; Grandjean et al., 2017; Lin et al., 2019). However, the mechanisms that govern the distribution and long elimination half-lives of PFAS in humans remain poorly understood (Olsen et al., 2007; Zhang et al., 2013). It has been debated that PFAS elimination in humans and rodents is primarily driven by renal clearance (Pizzurro et al., 2019; Niu et al., 2023). This study aims to uncover the poorly understood mechanisms driving renal clearance, including permeability and the role of organic ion transporters.

Long-chain PFAS like perfluorooctanoic acid (PFOA) and perfluorooctane sulfonic acid (PFOS) efficiently accumulate in humans due to their high gastrointestinal absorption and slow elimination, resulting in observed half-lives of 1.5-10 years (Calafat et al., 2007; Olsen et al., 2007; Kato et al., 2011; Zhang et al., 2013; Olsen et al., 2017). Because PFAS are generally resistant to phase-I and -II metabolism (Vandenheuvel et al., 1991), elimination primarily occurs via excretion. Therefore, urinary and fecal are considered to be dominant pathways for PFAS clearance from the body (Pizzurro et al., 2019), with renal clearance being considered a primary route of elimination in rats, monkeys, and humans (Butenhoff et al., 2004; Cui et al., 2010; Han et al., 2012; Zhang et al., 2013; Worley and Fisher, 2015). However, the molecular mechanisms that contribute to PFAS renal clearance are poorly understood, especially for emerging PFAS with

novel structures like fluorotelomers and sulfonamides.

Renal clearance is the rate at which a substance is removed from the blood and excreted by the kidneys in urine. It is driven by the combined processes of filtration, reabsorption, and secretion in the renal tubules (Tucker, 1981). Renal clearance occurs through uptake transporters, such as Organic Anion Transporters (OATs), which are localized at the basolateral membrane of renal proximal tubules and contribute to the transport of chemicals from the blood into the tubule. In addition, passive permeability can contribute to xenobiotic reabsorption from the urine and the kidney proximal tubules back into the blood (Tucker, 1981; Masereeuw and Russel, 2001; Varma et al., 2009; Varma et al., 2015). Because PFAS undergo little biotransformation (Pizzurro et al., 2019) and are excreted via the urine unchanged, OATs are considered likely mechanisms that contribute to renal clearance of PFAS (Lin et al., 2023; Niu et al., 2023). PFOA has been shown to be a high affinity substrate for rat OAT1 and OAT3 (Nakagawa et al., 2007), as well as human OAT4 (Louisse et al., 2023; Niu et al., 2023). A recent human-based physiologically based toxicokinetic (PBTK) model has suggested that transporter-mediated reabsorption is partly responsible for the long half-life of PFOA (Lin et al., 2023). When elucidating the overall renal clearance, other transporters expressed in the kidney such as OAT2 or Organic Cation Transporter 2 (OCT2) have not been examined, and human OATs have not been evaluated. Studies describing OAT4-mediated transport for different PFAS are also limited to seven PFAS with structural similarities (Nakagawa et al., 2009). Thus, PFAS with varying fluorinated carbon chain lengths and functional groups should be evaluated against human OATs to provide a broader mechanistic view and assessment of the relevance of renal clearance for the elimination of in humans as substrates and inhibitors.

In pharmaceutical sciences, various classifications have been developed to accelerate drug development and predict drug transporter interactions. Classification systems, such as the Extended Clearance Classification System (ECCS), could be helpful tools in predicting the elimination pathways for PFAS. The ECCS is a classification tool that was created to determine

clearance pathways for new chemical entities (mainly pharmaceuticals) based on molecular weight (MW), ionization, and permeability (Varma et al., 2009; Varma et al., 2015; El-Kattan and Varma, 2018). MW and ionization are predicted computationally, while permeability is often derived experimentally through using use of *in vitro* cell assays, such as the low efflux Madin-Darby canine kidney cells (MDCKII-LE) cell monolayer assays or parallel artificial membrane permeability assay (PAMPA) assay (Masungi et al., 2008). Passive permeability is an important parameter that contributes to renal clearance, with clearance decreasing as permeability increases. Apparent permeability (P_{app}) is one of the primary descriptors used in ECCS (Varma et al., 2009; Varma et al., 2012b). Despite being a critical parameter for estimating/understanding clearance, P_{app} values have only been arrived for a handful of PFAS using artificial planar lipid bilayers (Ebert et al., 2020). Although several PFAS and their chain length trends have been evaluated against several different renal transporters such as rat OAT1 and OAT3 (Weaver et al., 2010; Yang et al., 2010), PFAS-OAT interactions with regard to physicochemical properties (PC) important for predictive purposes have not yet been considered.

In this work, 14 PFAS were assessed for the following: apparent permeability (P_{app}) using MDCK-LE cell monolayer assays, and as substrates for the human renal transporters hOAT1, hOAT2, hOAT3, hOAT4, and hOCT2, and for hOAT1, hOAT3, and hOCT2 inhibition. The 14 study PFAS included 9 perfluoroalkyl carboxylates, 3 perfluoroalkyl sulfonates, 1 perfluoroalkyl sulfonamide, and 1 fluorotelomer sulfonate. Table S1 of the Supporting Information shows the study PFAS evaluated along with key physicochemical parameters (i.e. carbon chain length, MW, pKa, and logD). The fluorinated carbon chain lengths ranged from 3 to 11 (η_{pfc} = 3-11), the molecular weight ranged from 214.04 to 614.10 g/mol, and the logD ranged from 2.23 to 8.54. These PC properties were related to permeability and transporter interactions, and then evaluated against the established ECCS framework to identify likely excretion pathways (Varma et al., 2015).

2. Materials and Methods.

2.1 Chemicals and Reagents.

Perfluorobutanoic acid (PFBA), perfluoropentanoic acid (PFPA), perfluorohexanoic acid (PFHxA), perfluoroheptanoic acid (PFHpA), perfluorooctanoic acid (PFOA), perfluorononanoic acid (PFNA), perfluorodecanoic acid (PFDA), perfluoroundecanoic acid (PFUDA), perfluorododecanoic acid (PFDoDA), perfluorohexane sulfonic acid (PFHxS), perfluorooctanesulfonamide (PFOSA), and 6:2 fluorotelomer sulfonate (6:2FTS) were purchased from AccuStandard (New Haven, CT). Perfluorobutane sulfonic acid (PFBS) and perfluorooctane sulfonic acid (PFOS) were purchased from Sigma-Aldrich (St. Louis, MO). [^{14}C]-Metformin, [^{3}H]-PAH, and [^{3}H]-ES, were purchased from PerkinElmer Life Sciences (Boston, MA). BioCoat™ 96-well poly-D-lysine-coated plates were purchased from Corning. HEK293 cells stably transfected with human OAT1, OAT3, OAT4, and OCT2 were obtained from Dr. Kathleen Giacomini (University of California, San Francisco, CA) (Erdman et al., 2006; Zhang et al., 2006; Shima et al., 2010; Hsueh et al., 2016). HEK293 cells stably transfected with human OAT2 (tv-1 variant) were obtained from Dr. Ryan Pelis (Dalhousie University, Halifax, NS, Canada) (Cheng et al., 2012). MDCKII-LE cells that have been previously described for permeability assays were sourced from Pfizer Medicine Design (Groton, CT) (Di et al., 2011). Media components for HEK293 cell culture cells: Dulbecco's modified Eagle's medium (DMEM) high glucose, fetal bovine serum, minimum essential medium non-essential amino acids (MEM NEAA), gentamicin, GlutaMAX™, sodium pyruvate, penicillin and streptomycin solution were obtained from Thermo Fisher Scientific (Waltham, MA). The bicinchoninic acid (BCA) protein assay kit and NP-40 protein lysis buffer were also purchased from Thermo Fisher. Specific media components for MDCK cell culture: Minimum essential medium - alpha (MEM α), MEM NEAA, GlutaMAX™ and penicillin and streptomycin solution were purchased from Thermo Fisher. Ultima Gold XR scintillation fluid was purchased from PerkinElmer Life Sciences (Boston, MA).

2.2 Cell Culture.

HEK293 cells (wild-type and transfectants) were cultured using a base media of Dulbecco's modified Eagle's medium and supplemented with 10% fetal bovine serum, 1% 100 mM sodium pyruvate, 1% 100X GlutaMAX™, 1% 10 mg/mL gentamicin, and 1% 100X MEM NEAA. Cells were seeded in 96-well plates at a seeding density of 60,000-70,000 cells/well with a seeding volume of 0.1 mL/well, for a growth period of 2 days, maintained at 37°C, 5% CO_2, and 90% relative humidity. MDCKII-LE cells were cultured on Millicell-96 cell culture insert plates with 100 µL per insert well on the apical side at a seeding density of 25,000 cells/well with 32 mL of MEM α supplemented with 10% fetal bovine serum, 1% 100X MEM NEAA, 1% 100X GlutaMAX™, and 1% 10,000 units/mL of penicillin and 10,000 µg/mL of streptomycin in the single-well feeder tray on the basolateral side for 4 days, maintained at 37°C, 5% CO_2, and 90% relative humidity.

2.3 Permeability measurements using MDCKII-LE monolayers.

Apparent permeability (P_{app}) was determined as described previously with the addition of 0.4% bovine serum albumin (BSA) to the receiver compartment, to minimize non-specific binding to the plastic wells and plate (Di et al., 2011; Varma et al., 2012a; Fischer et al., 2018). Assay buffer was prepared at pH 7.4 using a custom ordered (Hanks' Balanced Salt Solution, HBSS) supplemented with 0.139 g/L calcium chloride, 25 mM D-glucose, 20 mM 4-(2-Hydroxyethyl)piperazine ethanesulfonic acid (HEPES), and 0.102 g/L magnesium chloride, and was also adjusted to pH 6.5. P_{app} assays were performed with 2 µM PFAS prepared in assay buffer with 1% DMSO yielding final PFAS concentrations well above analytical detection limits. PFAS were added to the donor wells and transport buffer containing 0.4% BSA was added to the receiver wells, to initiate the P_{app} assay. The plates were incubated at 37°C, and samples are taken from the donor compartment at 0 min and 90 min time-points, and the receiver compartment at a 90 min time-point, for analysis. P_{app} was measured at donor pH 6.5 or 7.4 and receiver at pH 7.4. P_{app} values for the PFAS evaluated were calculated as

$$P_{app} = \frac{dx/dt}{C_o \text{ x } A} \quad (1)$$

where dx is the change in PFAS mass in the receiver compartment, dt is the total incubation time, C_0 is the initial concentration in the donor compartment and A is the area of the cell culture surface area.

2.5 OAT1-4 and OCT2 Substrate Assays

The 14 study PFAS were screened according to previously described methods using control wild-type or human OAT and OCT transfectants (Mathialagan et al., 2017). HEK293 transport buffer were prepared at pH 7.4 using HBSS supplemented with 20 mM HEPES. Plated HEK293 cells were washed with transport buffer and pre-incubated with transport buffer for 5 minutes at 37°C, 5% CO_2, and 90% relative humidity, prior to the assay incubation. The assays were started with the addition of (0.1 mL) PFAS [1 µM], with and without pan-OAT inhibitor probenecid [1 mM], with a final concentration of 1% DMSO. Assay plates were placed on a heated shaker kept at 37°C and incubated for 3–4 minutes. The transport assays were stopped by removing the plates from the heated shaker, removal of the transport buffer by flipping/tapping the plate, and subsequently washed three times with ice-cold HBSS, with residual buffer being removed by aspiration. PFAS were extracted with 0.15 mL/well of 100% methanol containing internal standard to control for extraction efficiency. Cells were shaken for 45 minutes at room temperature, transferred to 96-well plates, centrifuged, and 0.1 mL/well of supernatant were transferred to new 96-well plate, and dried down under nitrogen gas. Samples were reconstituted in 50:50 acetonitrile:water and injected onto a liquid chromatography-tandem mass spectrometry (LC-MS/MS) system. The amount of PFAS uptake was calculated as analyte peak area ratio (PFAS peak area/internal standard peak area) as previously described.

The total protein per well, per cell type, was determined using a bicinchoninic acid protein assay per manufacturer directions. The protein samples were measured at an absorbance of 562

nm with the BioTek PowerWave HT, using the Gen5 software. Transporter uptake ratio was calculated as

$$\text{Uptake Ratio} = \left(\frac{\text{HEK293}-\text{Transfected area ratio}}{\text{mg protein}}\right) \Big/ \left(\frac{\text{HEK293}-\text{Wild type area ratio}}{\text{mg protein}}\right) \quad (2)$$

2.4 OAT1, 3, and OCT2 Inhibition Assay

OAT1 and 3, as well as OCT2 inhibition assays were performed as previously described (Mathialagan et al., 2017). OAT1 and 3 were tested because they are recognized as clinically relevant drug transporters (Burckhardt, 2012), indicating potential drug-drug interactions (DDIs) of substrates and PFAS. HEK293 transport buffer was prepared to pH 7.4 using HBSS supplemented with 20 mM HEPES. Plated HEK293 cells were washed with transport buffer and pre-incubated 30 minutes with PFAS at 37°C, 5% CO_2, and 90% relative humidity, prior to the assay incubation. The assays were started with the addition of 0.1 mL of the specific probe substrate for each specific transporter [(OAT1: [^{3}H]-PAH, 0.5 µM); (OAT3: [^{3}H]-ES, 0.1 µM); (OCT2: [^{14}C]-Metformin, 20 µM)] incubated for 3–4 minutes. Assay plates were placed on a heated shaker kept at 37°C throughout the incubation period. Transport activity was stopped by removing the plates from the heated shaker and washed three times with ice-cold HBSS. Radiometric probe substrates were extracted by treating the cells with 0.1 mL/well of lysis buffer (1% NP-40 in water) and shaken for 45 minutes at room temperature. Accumulated radioactivity was determined by mixing 0.08 mL of cell lysate with 0.2 mL of scintillation fluid. Radioactivity was measured and quantified on the Perkin Elmer MicroBeta^2 plate counter as counts per minute (CPM). Percent Activity was calculated as

$$Percent\ Activity = \frac{CPM_{\ probe+inhibitor} - CPM_{\ probe+control\ inhibitor}}{CPM_{\ probe} - CPM_{\ probe+control\ inhibitor}} \text{ x } 100 \quad (3)$$

Where the PFAS tested is the inhibitor and probenecid (OAT1 and OAT3) and quinidine (OCT2) are the control inhibitors. The estimated half-maximal inhibitory concentration (IC_{50}) for

the transporters was calculated in GraphPad Prism as

$$Percent\ Activity = Bottom + \frac{(Top - Bottom)}{1+10^{((LogIC_{50} - [Inhib]) * HillSlope)}} \text{ x } 100 \quad (4)$$

Note that probe substrate concentrations were consistently more than 10-fold lower than their corresponding Michaelis constant ([S]/Km < 0.1), therefore, IC50 approximate to equilibrium dissociation constant (Ki) of the PFAS, according to the Cheng-Prusoff Equation.**2.6 LC-MS/MS Quantification**

Samples were reconstituted in HPLC grade water:acetonitrile 50:50 (v/v), and vortexed for 1 minute. LC-MS/MS analysis was performed on a SCIEX Triple Quad 5500 mass spectrometer (SCIEX, Ontario, Canada) equipped with Turbo Ion Spray interface. The HPLC system consisted of an CTC PAL autosampler (LEAP Technologies, Morrisville, NC) equipped with a model 1290 binary pump (Agilent, Santa Clara, CA). All instruments were controlled and synchronized by SCIEX Analyst software (version 1.6.3), working in tandem with the ADDA software. The mobile phases were: 0.1% formic acid in water (mobile phase A) and 0.1% formic acid in acetonitrile (mobile phase B). The gradient for PFAS was maintained at 10% B for 0.8 min, followed by a 0.6-minute linear increase to 95% B, and kept at 95% B for 4 min, then a linear decrease to 10% for 0.1 minutes. The column was equilibrated at 5% B for 0.5 min. The total run time for each injection was 6 min. The chromatographic separation was carried out on a Phenomenex Kinetex C18 100Å 30 × 2.1 mm column, with a flow rate of 0.5 mL/min. The injection volume was 5 µL. Quadrupoles Q1 and Q3 were set on unit resolution, and the mass over charge (m/z) of the analytes are shown in Supplementary Table S1. Multiple-reaction-monitoring (MRM) mode, using specific precursor/product ion transitions, was used for quantification. Data processing was performed using SCIEX Analyst software (version 1.6.3).

2.7 Statistical Analysis

Standard statistical tests were used to analyze uptake differences between groups

(transfected *vs* wild type) and uptake ratio differences between groups (with *vs* without inhibitor). A parametric t-test (unpaired, one-tailed, unequal variance) was employed to determine the significance. All statistical analysis tests were evaluated on SAS version 9.4.

3. Results

3.1 PFAS Membrane Permeability.

The passive permeability determined in MDCKII cell monolayers at pH 7.4 for the 14 PFAS ranged from 0.71 x 10^{-6} to 41 x 10^{-6} cm/sec (Fig. 1, Table S3). The legacy PFOA and PFOS had P_{app} values of 1.5 and 14 x 10^{-6} cm/sec, respectively. Low permeability, as defined as P_{app} <5.0 cm/s (Varma et al., 2015), was observed for compounds with MW <450 and logD <6.3, whereas P_{app} increased as MW and logD increased for perfluoroalkyl carboxylates, perfluoroalkyl sulfonates, and PFOSA (Figs. 1A and B). Interestingly, P_{app} were similar between pH 7.4 and 6.5 for all PFAS but PFOSA (Fig. S1).

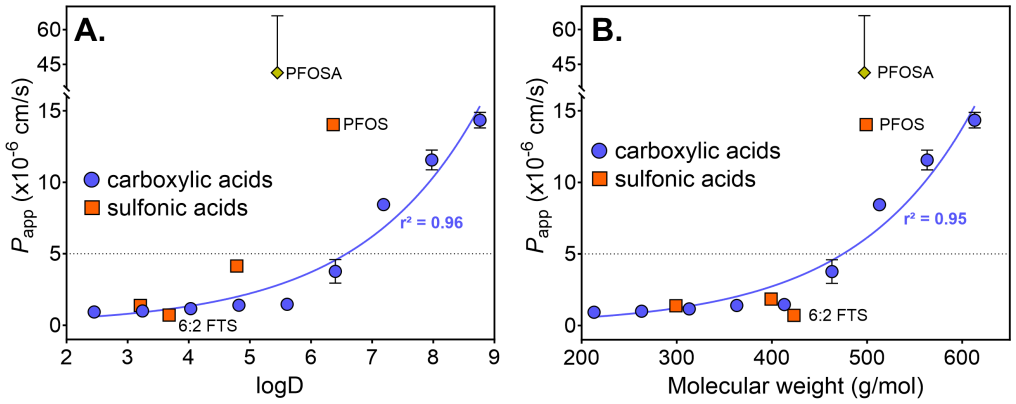

Figure 1: LogD (A) and molecular weight (B) plotted against apparent permeability P_{app} of PFAS at pH 7.4. PFAS were grouped into carboxylic and sulfonic acids and PFOSA (sulfonamide). PFOSA and PFOS is highlighted due to their high permeability. 6:2 FTS is highlighted for its low permeability. The solid blue lines are exponential growth fits for the carboxylic acids, and the goodness-of-fit is reported (r^2). The dotted line is the permeability cut-off of 5 x 10^{-6} as applied in the ECCS framework (Varma et al., 2015).

3.2 hOAT1, hOAT3, and hOAT4 substrate activities.

The 14 PFAS were next screened as potential substrates for hOAT 1–4 and hOCT2, which are uptake transporters expressed in human kidney proximal tubules. Overall, multiple PFAS had uptake ratios greater than 2-fold (Fig. 2, Fig. S2), indicating they are likely hOAT1, hOAT3, and hOAT4 substrates according to ECCS (Varma et al., 2015). For 6:2 FTS and PFHxA, the hOAT1

uptake ratio was ~15-fold and ~2-fold higher than the control, suggesting that PFHxA and 6:2 FTS are substrates for hOAT1. PFHpA, PFOA, and PFBS had uptake ratios that were 5-60% higher than controls, with PFBS>PFOA>PFHpA>PFPA – suggesting that they could have weak interactions with hOAT1. hOAT1 uptake ratios for PFNA, PFDA, PFUDA, PFDoDA, PFHxS, PFOS, and PFOSA were similar to control transfectants. None of the 14 PFAS screened had uptake ratios above control for hOAT2 (Fig. 2, Fig. S2B).

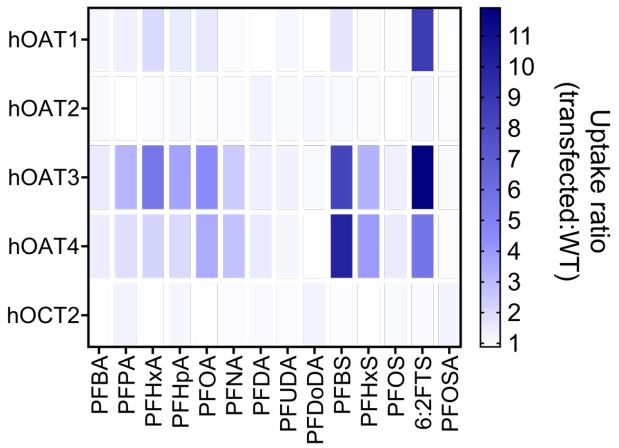

Figure 2: Heat map of PFAS substrate activity of PFAS against human OAT1, OAT2, OAT3, and OAT4 expressed in human kidney proximal tubules. The color code indicates uptake ratios (transfected vs. wild-type cells) from 1 (baseline, white) to 11.9 (highest value, dark blue).

For hOAT3, 12/14 PFAS had uptake ratios >20% of the control, with 8/14 PFAS exceeding the 2-fold threshold (Fig. 2., Fig. S3). PFPA, PFHxA, PFHpA, PFOA, PFNA, PFBS, PFHxS, and 6:2 FTS had uptake ratios that were ~2.5-12 fold higher than mock transfected controls, indicating that they are probable substrates for hOAT3 (Varma et al., 2015). The uptake ratios for PFBA, PFDA, and PFOS were 30-50% higher than mock transfectants, suggesting minimal to modest potential interaction with hOAT3. PFUDA, PFDoDA and PFOSA had uptake ratios similar to control. 9 out of 14 PFAS had uptake ratios that were higher in the hOAT4 transfectants than controls (Fig, 2, Fig. S2D). PFOA, PFNA, PFBS, PFHxS, and 6:2 FTS had uptake ratios greater than 2-fold, indicating that they are probable hOAT4 substrates. PFHxA, PFHpA, and PFOS had uptake ratios that were ~20% above controls, indicating weak interactions with hOAT4. hOCT2

was also screened for PFAS uptake (Fig. 2, Fig. S3). 12 of the 14 PFAS evaluated had uptake rations that were similar to control. PFDoDA and PFOSA had minimal increased uptake ratios that were ~10% higher than mock transfectant controls. Overall, PFAS had minimal to no interactions with hOCT2 and the tested PFAS are not considered to be substrates.

As a follow-up analysis and based on the ≥2-fold increase in uptake as compared to the empty vector cell (FDA, 2020), additional testing was performed for the PFAS that were classified as probable OAT substrates. Therefore, uptake of these PFAS was characterized in the presence of probenecid, a known OAT inhibitor. Fig. 3 illustrates hOAT-mediated uptake of PFHxA (~2 fold) and 6:2 FTS (~4 fold), that was markedly reduced by probenecid co-treatment. Fig. 3B illustrates hOAT3-mediated uptake of PFPA, PFHxA, PFHpA, PFOA, PFNA, PFBS, PFHxS, and 6:2 FTS by 2.5-15-fold, which was markedly inhibited by probenecid cotreatment. Lastly, hOAT4-mediated uptake of PFPA, PFHxA, PFHpA, PFOA, PFNA, PFBS, and 6:2 FTS (~2-4 fold higher) was effectively inhibited by probenecid co-treatment. PFHxS uptake was not inhibited by probenecid, suggesting a potentially novel interaction with hOAT4.

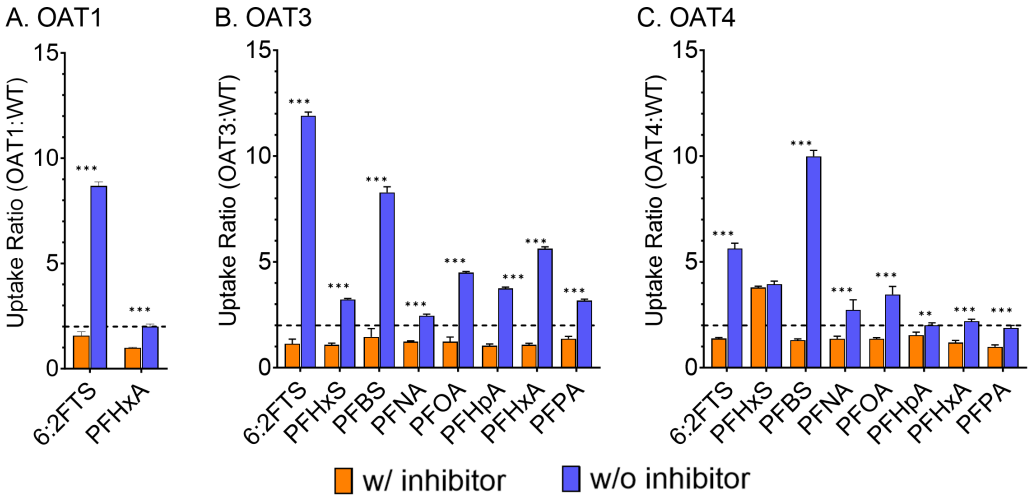

Figure 3: Substrate uptake ratios of PFAS against human (A) OAT1, (B) OAT3, and (C) OAT4, with (w/) and without (w/o) OAT-specific inhibitor probenecid [1mM]. Significant inhibition was shown against all PFAS transporter combination (t-test, ***: p<0.001, **: p <0.01), except for PFHxS and OAT4.

3.4 PFAS Renal Transporter Inhibition

As an additional evaluation for OAT-PFAS interactions, PFAS were screened as potential inhibitors of hOAT1 and hOAT3 mediated uptake of para-aminohippurate (PAH) and estrone-sulfate (ES), respectively, and hOCT2 mediated uptake of quinidine. hOAT1 and hOAT3 were selected because their function in regard to xenobiotic uptake of PAH (hOAT1 probe) and ES (hOAT3 probe) into the renal tubule is well accepted and they are known to contribute to xenobiotic disposition, as well as clearance. Figs. S4–7 illustrate half-maximal inhibitory concentrations (IC_{50}) for 14 PFAS for OAT1-, OAT3-, and OCT2-mediated transport of prototypical substrates. PFHxA, PFHpA, and PFOA showed moderate potency for hOAT1-transporter inhibition (Figs. 4, S4, S7). PFHxA, PFHpA, and PFOA had IC_{50} ranges of 51.4 µM–166.4 µM while 6:2 FTS showed the most potent inhibition against hOAT1 with an IC_{50} value of 6.7 µM.

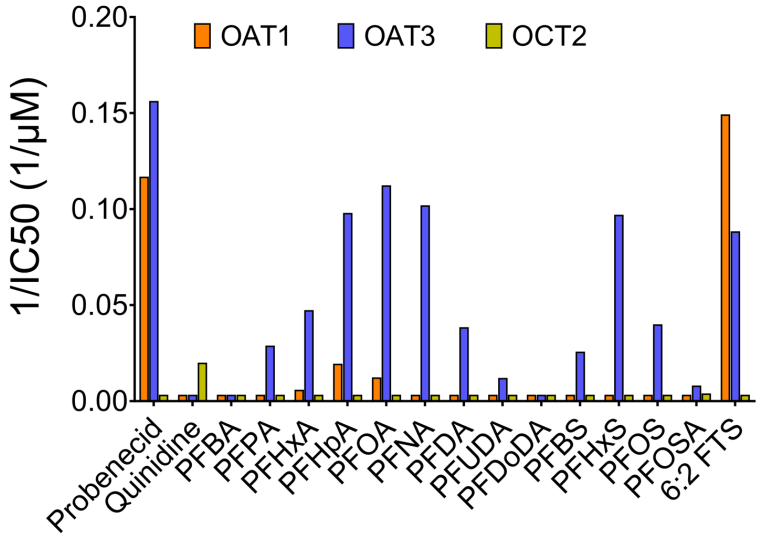

Figure 4: Reciprocals of 50% inhibitory concentrations (IC50, 1/µM) for the study PFAS against hOAT1, hOAT3, and hOCT2 mediated uptake of prototypical substrates. Probenecid and quinidine were tested as control inhibitors for OATs and OCT, respectively. IC50 of >300 µM were set to 1/300 µM in the graph to indicate the baseline.

The tested PFAS showed more potent hOAT3-transporter inhibition as compared to hOAT1, with PFOA (IC_{50}: 8.9 µM), PFNA (IC_{50}: 9.8 µM), PFHpA (IC_{50}: 10.2 µM), PFHxS (IC_{50}: 10.3 µM), and 6:2FTS (IC_{50}: 11.3 µM) showing strong inhibition of probe uptake. Several other PFAS showed

moderate potency for OAT3 inhibition as PFPA, PFHxA, PFDA, PFUDA, PFBS, PFOS, and PFOSA had IC_{50} ranges of 21.1 μM – 123.3 μM (Fig. S5). Potent inhibition against hOCT2 was not observed for this set of PFAS, with PFOSA (IC_{50}: 244.7 μM) indicating weak hOTC2 inhibition (Fig. S6). Probenecid, a potent hOAT1 and hOAT3 competitive inhibitor, has displayed IC_{50} values of 8.6 and 6.4 μM, respectively. For hOAT3, several of the PFAS tested showed potency similar to that of probenecid. Notably, 6:2 FTS (IC50: 6.7 μM) showed more potency in hOAT1 than probenecid (IC50: 8.6 μM). These results illustrate that hOAT1 (PAH) and hOAT3 (ES) specific probes were inhibited by the addition of PFAS, indicating a transporter interaction with PFAS. Moreover, there were 4 PFAS that showed hOAT1 inhibitory effects, whereas there were 12 PFAS that showed hOAT3 inhibitory effects within our overall 14 PFAS dataset. 85% of the PFAS herein showed some level of inhibition against hOAT1 and hOAT3 mediated transport of probenecid, with the smaller PFBA and larger PFDoDA being the only exceptions.

3.5 Application of the ECCS Framework

The ECCS framework (Varma et al., 2015), developed to predict clearance mechanisms in drug discovery compounds, considers three important parameters: MW, ionization, and permeability, of which permeability is the key component to determine whether a compound will likely be renally cleared. Renal clearance is expected to decrease with increased lipophilicity; therefore, it is also expected for an increased permeability to lead to lower renal clearance (Varma et al., 2012a). Within the ECCS framework, compounds are further categorized using cutoffs for MW: high (> 400) or low (≤ 400); ionization: acids/zwitterions or bases/neutrals; and permeability: high (≥ 5.0 x 10^{-6} cm/sec) or low (< 5.0 x 10^{-6} cm/sec) (Varma et al., 2015; El-Kattan and Varma, 2018). Full ECCS categorization of PFAS within this set shown in Table 1. 14 PFAS were categorized into 3 of the 6 classes: Class 1B (high permeable, MW > 400, acid): PFDA, PFUDA, PFDoDA, PFOS, PFOSA; Class 3A (low permeable, MW ≤ 400, acid): PFBA, PFPA, PFHxA, PFHpA, and PFBS; and Class 3B (low permeable, MW > 400, acid): PFNA, PFOA, PFHxS, and 6:2FTS. The main

333 determinants of a compound's renal clearance are its permeability and renal transporter activity.
334 Therefore, this ECCS classification, although mainly for the purposes of categorizing clearance
335 pathways, i.e., hepatobiliary vs renal clearance, also gives mechanistic insight for which
336 transporters may interact with specific PFAS. For example, PFAS within the class 3A category
337 (low permeable, MW ≤ 400, acid) would be expected to interact with OAT1, OAT2, OAT3, OAT4.
338 Class 3B (low permeable, MW > 400, acid) would be expected to interact with OAT3, and class
339 1B compounds (high permeable, MW > 400, acid) would have limited interaction with renal
340 transporters (Varma et al., 2015). None of the PFAS are categorized as Class 1A, 2 or 4 as the
341 compounds tested with MW ≤ 400 all showed low permeability (Class 1A) and no bases were
342 within this PFAS set (Class 2 and 4). Therefore, PFAS within this dataset were not expected to
343 interact with OCT2.

344 **Table 1.** PFAS Extended Clearance Classification System (ECCS) class alongside their
345 corresponding molecular weight (g/mol), apparent permeability (Papp), and ionization.
346 Characterization of OAT1, 2, 3, 4 and OCT2 denoted with a "+" to denote a threshold of ≥ 2-fold
347 has been met and considered a substrate for the transporter.

PFAS	Molecular weight	Ph 7.4 A-B P_{app}	Ionization	ECCS Class	Transporter Uptake Ratio				
	(g/mol)	(x 10^{-6} cm/sec)			OAT1	OAT2	OAT3	OAT4	OCT2
Perfluoroalkyl Carboxylates									
PFBA	214.04	0.93	Acid	3A					
PFPA	264.05	0.99	Acid	3A			+		
PFHxA	314.05	1.16	Acid	3A	+		+	+	
PFHpA	364.06	1.40	Acid	3A			+	+	
PFOA	414.07	1.46	Acid	3B			+	+	
PFNA	464.08	3.77	Acid	3B			+	+	
PFDA	514.08	8.44	Acid	1B					
PFUDA	564.09	11.56	Acid	1B					
PFDoDA	614.1	14.35	Acid	1B					
Perfluoroalkyl Sulfonates									
PFBS	300.1	1.38	Acid	3A			+	+	
PFHxS	400.12	4.14	Acid	3B			+	+	
PFOS	500.13	14.04	Acid	1B					
Fluorotelomer Sulfonates									
6:2FTS	427.98	0.71	Acid	3B	+		+	+	
Perfluoroalkyl Sulfonamides									
PFOSA	499.14	41.39	Acid	1B					

348

4. Discussion

With thousands of PFAS described and countless numbers of novel structures, there is an urgent need to understand and predict mechanisms for bioaccumulation and clearance in humans and preclinical toxicology models (i.e. rats, mice, monkeys, zebrafish) through associating physicochemical properties with mechanisms of clearance and elimination. In humans, rodents, and monkeys, PFAS are often detected in urine (Andersen et al., 2006; Zhang et al., 2013), indicating renal clearance as a mechanism of elimination. Renal clearance is determined by glomerular filtration, tubular secretion, and reabsorption. Reabsorption of xenobiotics along the nephron is mainly driven by passive permeability, due to the high concentration gradient of the compounds following the water reuptake process (Sun et al., 2006; Fagerholm, 2007). Tubular secretion is mediated via OATs-with facilitated transport of substrates from the blood to the tubule via OAT1 and OAT3 localized to the basolateral membrane and then excretion via OAT4 or ATP-Binding Cassette (ABC) efflux transporters.

The 14 PFAS were screened for permeability as a first step. In this study, permeability was tested at pH 7.4 and 6.5. The pH 6.5:7.4 gradient was tested to mimic the transition of urinary to blood pH, and a no gradient condition (pH 7.4:7.4) was used to classify the PFAS according to ECCS (Varma et al., 2015). Under both physiological pH conditions, P_{app} increased as lipophilicity increased for carboxylates and sulfonates (Figs. 1 and S1). This positive association between logD and P_{app} is consistent with what is observed with pharmaceuticals (Chan and Stewart, 1996; Oja et al., 2019). Among the 14 PFAS evaluated, PFOSA (logD: 5.5) stood out with a relatively high permeability of 41.4 x 10^{-6} cm/sec at pH 7.4. Unlike the other PFAS, PFOSA was the only weak acid evaluated, with a pKa of 6.24. The pKa range of the other PFAS evaluated ranged from -0.17 to 2.50. This relatively high permeability may be because weak acids, such as PFOSA, have a higher fraction of neutral species ($f_{neutral}$ [pH 6.5] = 35%) that are not ionized and more readily available to cross the membrane as compared to stronger acids such as PFOA $f_{neutral}$ [pH 6.5] = <0.001%) (Avdeef and Testa, 2002). At pH 7.4, the neutral fraction of PFOSA is ~6%, which

explains why P_{app} of PFOSA was ~2 times higher at pH 6.5 than at pH 7.4.

Next, the 14 PFAS were evaluated as substrates for human transporters relevant to renal excretion. High permeable Class 1B compounds have shown to be more susceptible to renal reabsorption and less susceptible to renal uptake transporters, further limiting their ability to be cleared via the urine. The PFAS compounds in Classes 3A and 3B, which have low permeability, may interact with renal uptake transporters on the basolateral side of the kidney proximal tubules, such as hOAT1, hOAT2, or hOAT3, where acidity is one of the principal determinants of substrate activity (Inui et al., 2000; Launay-Vacher et al., 2006; Varma et al., 2015; El-Kattan and Varma, 2018). Based on this established framework, we expected the compounds with low permeability in our set (Classes 3A and 3B) to have renal transporter activity and urinary excretion. With the exception of PFBA, all Class 3 PFAS in our set are considered hOAT1 and/or hOAT3 substrates (Figs. 2-4). Although PFBA did not reach the 2-fold cut-off, PFBA still showed a statistically significant hOAT3 uptake ratio of 1.5, which could be considered a weak substrate. In line with expectations, no Class 1B PFAS were shown to be substrates for hOAT1-3, using the 2-fold uptake ratio cut-off. This data suggests that although structurally diverse, PFAS follow the basic physicochemical framework predictions for renal transporter activity, similar to pharmaceutical compounds.

Previous *in vitro* studies have shown PFHpA, PFOA, PFNA, and PFDA to be substrates of rat OAT1 and/or OAT3 (Weaver et al., 2010) and PFOA had a high affinity for human OAT1 and OAT3 (Nakagawa et al., 2008). Agreeing with these studies, our *in vitro* assays suggest PFHpA, PFOA, and PFNA as substrates of hOAT1 and/or hOAT3, and PFDA as a weak substrate of hOAT3. Similarly, Weaver et al. (2010) also did not see any activity for PFDA against rat OAT1. This data aligns with the ECCS characteristics of PFDA as Class 1B compound with limited expected OAT1 or OAT3 substrate activity. OCT2 is another high interest renal transporter tested in our study. However, because basicity is one of the physicochemical attributes of OCT2 substrates (Ullrich, 1997), very limited OCT2 substrate or inhibition activity was seen for the PFAS

401 tested (Figs. 2-4). Collective findings suggest an association of certain PFAS with OATs, which
402 may contribute to their active renal secretion in humans (Pizzurro et al., 2019). All Class 3
403 compounds in our PFAS set showed inhibitory activity against hOAT1 and/or hOAT3 (Fig. 4), with
404 the exception of PFBA, while only PFOSA (a weak acid) showed minor inhibitory activity against
405 OCT2. Understanding the inhibitory nature of PFAS is important, as inhibition of the evaluated
406 transporters may lead to drug-drug interactions (International Transporter Consortium et al.,
407 2010). Considering the high plasma protein binding of PFAS (>99.99% bound, Alesio et al. (2022)
408 and comparing their IC50 values (>6.7μM) with blood levels found in individuals with significant
409 occupational exposure of >5μM, such as ski technicians (Lucas et al., 2023), the likelihood of
410 PFAS reaching unbound concentrations capable of inhibiting OAT1 or OAT3 and causing drug-
411 drug interactions appears to be low.

412 OAT2 is localized in the kidney and has shown to contribute to the renal active tubular
413 secretion of several xenobiotics and endogenous compounds (Lepist et al., 2014; Mathialagan et
414 al., 2017; Shen et al., 2017; Mathialagan et al., 2020; Ryu et al., 2022). OAT2 plays a role in the
415 mediated uptake for Class 1A substrates (high permeable and low MW acids/zwitterions) (Kimoto
416 et al., 2018), and other reports have shown they can also transport Class 4 (low permeable
417 bases/neutrals) compounds (El-Kattan and Varma, 2018). Our PFAS set did not have any
418 compounds classified as Class 1A or 4. Moreover, no PFAS in our set had any uptake activity
419 against OAT2. Our results were consistent to previous rat OAT2 results against PFHpA, PFOA,
420 PFNA, and PFDA (Weaver et al., 2010), and human OAT2 against PFOA (Nakagawa et al., 2008),
421 where both studies showed no uptake activity.

422 Several studies have demonstrated that urinary excretion is the primary route of
423 elimination for PFOA (low permeable Class 3B PFAS) in rats and monkeys, with a rat renal
424 clearance of ~50-80%, compared to the total clearance in rats (Ohmori et al., 2003; Butenhoff et
425 al., 2004; Harada et al., 2005; Cui et al., 2009; Cui et al., 2010). PFAS with shorter fluorinated
426 carbon chain length (η_{pfc}), such as PFBA and PFHxA, were shown to have much faster renal

elimination rates in several mammalian species (Chang et al., 2008; Chengelis et al., 2009). Further η_{pfc}-dependent trends in rat renal elimination have been reported for PFHpA, PFOA, PFNA, and PFDA (Kudo et al., 2001; Ohmori et al., 2003). The study by Zhang et al. (2013) showed that as η_{pfc} increases for perfluoroalkyl carboxylic acids - PFCAs (PFHpA, PFOA, PFNA, PFDA, and PFUDA), the human renal clearance decreases, where PFHpA (η_{pfc} = 6), had a ~10-fold higher renal clearance rate than PFUDA (η_{pfc} = 10). The trend observed in both animal and human data, indicating that PFCAs with shorter η_{pfc} have increased renal clearance, further validates our study's findings that an increase in η_{pfc} length of PFCAs is also associated with increased permeability (Fig. 1). Although the apparent relationship between η_{pfc} and renal clearance is significant in several of these studies, we believe that logD and permeability are the main drivers behind this renal clearance trend, more so than η_{pfc} alone.

OAT4, a renal transporter located on the apical side of the kidney proximal tubules, is known to play a role in the reabsorption of compounds from the tubules back into the blood (Nigam et al., 2015). Nakagawa et al. (2009) demonstrated OAT4-mediated transport activity of PFOA was similar to what we saw in our study. We further assessed, and have shown that several PFAS with low permeabilities, such as PFHxA, PFHpA, PFOA, PFNA, PFBS, PFHxS, and 6:2 FTS, are strong substrates of OAT4. Investigation into the inhibition of OAT4 by PFAS should be conducted in future studies to further understand its implications in drug-drug interactions. Of note, at the time of this study, no physicochemical property comparison work has been done for OAT4. There are several overlaps between OAT1, OAT3, and OAT4 for our PFAS set, however, further understanding of physicochemical predictors is required. Although several of these PFAS are expected to be renally cleared, one of the likely mechanisms behind their slow renal clearance and long elimination half-lives may be due to reabsorption via OAT4. Interestingly, although PFHxS is bound to serum proteins similarly strong as PFOS (Alesio et al., 2022; Fischer et al., 2024), less permeable and more renal uptake transporter OAT1-3 activity than PFOS (Figs. 1 and

2), PFHxS showed a lower renal clearance (Pizzurro et al., 2019). This suggests there may be additional mechanisms, outside of permeability and uptake transporter activity, related to the overall renal clearance for PFAS. Of note, PFHxS was a strong substrate of OAT4 (Figs. 2 and S2C), while PFOS was a relatively weak substrate, with a fold difference in uptake ratio of ~2.5 between the two PFAS. This mechanism of OAT4 transporter reuptake could be one of the underlying reasons for the differences in renal clearance, as suggested by Lin et al. (2023) in their PBTK model. A recent NHANES analysis by Ducatman et al. (2021) has shown that probenecid, a known OAT inhibitor, does not significantly change PFAS (PFHxS, PFOA, PFOS, and PFNA) serum concentrations. Although, the sample sizes were small within data set, it indirectly suggests that OATs may not play a major role in the overall renal clearance of PFAS in humans, and/or other mechanisms such as permeability are involved in the reabsorption of the PFAS compounds back into the blood. Future studies should investigate the interaction of PFAS with other drug efflux transporters expressed in human kidneys, such as OATP4C1 (Drozdzik et al., 2021), MDR1/P-gp, BCRP/Bcrp, MRP2/Mrp2 and MRP3/Mrp3 (Fallon et al., 2016).

5. Conclusion

Our study presents the first set of permeability data for PFAS in physiologically relevant *in vitro* conditions with human cell lines. On the basis of our P_{app} data and physicochemical properties of the PFAS (MW, logD, ionization), we classified the study PFAS according to their potential for renal clearance. We observed a clear relationship between lipophilicity and P_{app}, and PFAS with low permeability showed stronger interactions with renal transporters. Several PFAS tested in these studies demonstrated strong interactions with renal transporters. Of particular note is 6:2 FTS, which showed low permeability but strong renal transporter interactions in both substrate and inhibition assays. 6:2 FTS is an emerging PFAS used as alternative to the phased-out PFOA and PFOS, and our results indicate that 6:2 FTS exposure in humans will be strongly driven by renal transporters. These trends indicate the necessity to screen emerging PFAS with more

complex structures for their interactions with renal transporters for risk assessment purposes. OAT4-mediated tubular reabsorption may be the driver of the long elimination half-lives observed for PFAS with relatively short fluorinated carbon chains, such as PFHxS. The expanded toxicokinetic data set for P_{app} and renal transporters provided in this paper improved our understanding of the role of renal secretion and reabsorption in the overall elimination of PFAS in humans. Overall, our PFAS uptake data aligns well with the transporter ECCS framework predictions, and validates that permeability, MW, and ionization can be useful for PFAS transporter activity predictions (El-Kattan and Varma, 2018). This study utilized *in vitro* assays, necessitating validation of our findings through in vivo experiments with rodents while considering for species-species differences in transporter expression (Floerl et al., 2022). Further *in vitro* and *in vivo* renal clearance-based studies will further validate the ECCS and total clearance predictions for PFAS in humans based on *in vitro* permeability and renal transporter assays. The toxicokinetic data provided in our study is useful input data for physiologically-based toxicokinetic (PBTK) models to investigate the relevance of P_{app} and renal transporters in the overall distribution and elimination of PFAS in humans.

6. Acknowledgements

The authors would like to thank dissertation committee members, Drs. Roberta King, Rainer Lohmann, and Brenton DeBoef for their insightful comments as the project was being developed.

7. Funding

This work was supported by National Institute of Health Grant number P42ES027706 (R. Lohman, principal investigator; A. Slitt, Project 3 Lead). The funders had no role in study design, data collection and analysis, decision to publish, or preparation of the manuscript. S. Ryu was a recipient of the Choi Scholarship from the University of Rhode Island.

References

Alesio, J.L., Slitt, A., Bothun, G.D., 2022. Critical new insights into the binding of poly- and perfluoroalkyl substances (PFAS) to albumin protein. Chemosphere 287, 131979.

Andersen, M.E., Clewell, H.J., Tan, Y.-M., Butenhoff, J.L., Olsen, G.W., 2006. Pharmacokinetic modeling of saturable, renal resorption of perfluoroalkylacids in monkeys—Probing the determinants of long plasma half-lives. Toxicology 227, 156-164.

Avdeef, A., Testa, B., 2002. Physicochemical profiling in drug research: a brief survey of the state-of-the-art of experimental techniques. Cell Mol Life Sci 59, 1681-1689.

Barry, V., Winquist, A., Steenland, K., 2013. Perfluorooctanoic Acid (PFOA) Exposures and Incident Cancers among Adults Living Near a Chemical Plant. Environ Health Persp 121, 1313-1318.

Burckhardt, G., 2012. Drug transport by Organic Anion Transporters (OATs). Pharmacol Ther 136, 106-130.

Butenhoff, J.L., Kennedy, G.L., Hinderliter, P.M., Lieder, P.H., Jung, R., Hansen, K.J., Gorman, G.S., Noker, P.E., Thomford, P.J., 2004. Pharmacokinetics of perfluorooctanoate in cynomolgus monkeys. Toxicological Sciences 82, 394-406.

Calafat, A.M., Wong, L.Y., Kuklenyik, Z., Reidy, J.A., Needham, L.L., 2007. Polyfluoroalkyl chemicals in the US population: Data from the National Health and Nutrition Examination Survey (NHANES) 2003-2004 and comparisons with NHANES 1999-2000. Environ Health Persp 115, 1596-1602.

Chan, O.H., Stewart, B.H., 1996. Physicochemical and drug-delivery considerations for oral drug bioavailability. Drug Discov Today 1, 461-473.

524 Chang, S.C., Das, K., Ehresman, D.J., Ellefson, M.E., Gorman, G.S., Hart, J.A., Noker, P.E.,
525 Tan, Y.M., Lieder, P.H., Lau, C., Olsen, G.W., Butenhoff, J.L., 2008. Comparative
526 pharmacokinetics of perfluorobutyrate in rats, mice, monkeys, and humans and relevance to
527 human exposure via drinking water. Toxicological Sciences 104, 40-53.

528 Cheng, Y., Vapurcuyan, A., Shahidullah, M., Aleksunes, L.M., Pelis, R.M., 2012. Expression of
529 organic anion transporter 2 in the human kidney and its potential role in the tubular secretion of
530 guanine-containing antiviral drugs. Drug Metab Dispos 40, 617-624.

531 Chengelis, C.P., Kirkpatrick, J.B., Myers, N.R., Shinohara, M., Stetson, P.L., Sved, D.W., 2009.
532 Comparison of the toxicokinetic behavior of perfluorohexanoic acid (PFHxA) and
533 nonafluorobutane-1-sulfonic acid (PFBS) in cynomolgus monkeys and rats. Reprod Toxicol 27,
534 400-406.

535 Cui, L., Liao, C.Y., Zhou, Q.F., Xia, T.M., Yun, Z.J., Jiang, G.B., 2010. Excretion of PFOA and
536 PFOS in Male Rats During a Subchronic Exposure. Arch Environ Con Tox 58, 205-213.

537 Cui, L., Zhou, Q.F., Liao, C.Y., Fu, J.J., Jiang, G.B., 2009. Studies on the Toxicological Effects
538 of PFOA and PFOS on Rats Using Histological Observation and Chemical Analysis. Arch
539 Environ Con Tox 56, 338-349.

540 Darrow, L.A., Stein, C.R., Steenland, K., 2013. Serum Perfluorooctanoic Acid and
541 Perfluorooctane Sulfonate Concentrations in Relation to Birth Outcomes in the Mid-Ohio Valley,
542 2005-2010. Environ Health Persp 121, 1207-1213.

543 Di, L., Whitney-Pickett, C., Umland, J.P., Zhang, H., Zhang, X., Gebhard, D.F., Lai, Y., Federico,
544 J.J., 3rd, Davidson, R.E., Smith, R., Reyner, E.L., Lee, C., Feng, B., Rotter, C., Varma, M.V.,
545 Kempshall, S., Fenner, K., El-Kattan, A.F., Liston, T.E., Troutman, M.D., 2011. Development of
546 a new permeability assay using low-efflux MDCKII cells. J Pharm Sci 100, 4974-4985.

547 Drozdzik, M., Drozdzik, M., Oswald, S., 2021. Membrane Carriers and Transporters in Kidney
548 Physiology and Disease. Biomedicines 9, 426.

549 Ducatman, A., Luster, M., Fletcher, T., 2021. Perfluoroalkyl substance excretion: Effects of
550 organic anion-inhibiting and resin-binding drugs in a community setting. Environ Toxicol
551 Pharmacol 85, 103650.

552 Ebert, A., Allendorf, F., Berger, U., Goss, K.U., Ulrich, N., 2020. Membrane/Water Partitioning
553 and Permeabilities of Perfluoroalkyl Acids and Four of their Alternatives and the Effects on
554 Toxicokinetic Behavior. Environmental Science & Technology 54, 5051-5061.

555 El-Kattan, A.F., Varma, M.V.S., 2018. Navigating Transporter Sciences in Pharmacokinetics
556 Characterization Using the Extended Clearance Classification System. Drug Metabolism and
557 Disposition 46, 729-739.

558 Erdman, A.R., Mangravite, L.M., Urban, T.J., Lagpacan, L.L., Castro, R.A., de la Cruz, M.,
559 Chan, W., Huang, C.C., Johns, S.J., Kawamoto, M., Stryke, D., Taylor, T.R., Carlson, E.J.,
560 Ferrin, T.E., Brett, C.M., Burchard, E.G., Giacomini, K.M., 2006. The human organic anion
561 transporter 3 (OAT3; SLC22A8): genetic variation and functional genomics. Am J Physiol Renal
562 Physiol 290, F905-912.

563 Fagerholm, U., 2007. Prediction of human pharmacokinetics - renal metabolic and excretion
564 clearance. Journal of Pharmacy and Pharmacology 59, 1463-1471.

565 Fallon, J.K., Smith, P.C., Xia, C.Q., Kim, M.-S., 2016. Quantification of Four Efflux Drug
566 Transporters in Liver and Kidney Across Species Using Targeted Quantitative Proteomics by
567 Isotope Dilution NanoLC-MS/MS. Pharmaceutical Research 33, 2280-2288.

FDA, 2020. In Vitro Drug Interaction Studies — Cytochrome P450 Enzyme- and Transporter-Mediated Drug Interactions Guidance for Industry. in: Administration, U.D.o.H.a.H.S.F.a.D. (Ed.).

Fei, C.Y., McLaughlin, J.K., Tarone, R.E., Olsen, J., 2007. Perfluorinated chemicals and fetal growth: A study within the Danish National Birth Cohort. Environ Health Persp 115, 1677-1682.

Fischer, F.C., Cirpka, O.A., Goss, K.U., Henneberger, L., Escher, B.I., 2018. Application of Experimental Polystyrene Partition Constants and Diffusion Coefficients to Predict the Sorption of Neutral Organic Chemicals to Multiwell Plates in in Vivo and in Vitro Bioassays. Environ Sci Technol 52, 13511-13522.

Fischer, F.C., Ludtke, S., Thackray, C., Pickard, H.M., Haque, F., Dassuncao, C., Endo, S., Schaider, L., Sunderland, E.M., 2024. Binding of Per- and Polyfluoroalkyl Substances (PFAS) to Serum Proteins: Implications for Toxicokinetics in Humans. Environmental Science & Technology 58, 1055-1063.

Floerl, S., Kuehne, A., Hagos, Y., 2022. Functional characterization and comparison of human and mouse organic anion transporter 1 as drugs and pesticides uptake carrier. European Journal of Pharmaceutical Sciences 175, 106217.

Geiger, S.D., Xiao, J., Ducatman, A., Frisbee, S., Innes, K., Shankar, A., 2014. The association between PFOA, PFOS and serum lipid levels in adolescents. Chemosphere 98, 78-83.

Giesy, J.P., Kannan, K., 2001. Global distribution of perfluorooctane sulfonate in wildlife. Environ Sci Technol 35, 1339-1342.

588 Grandjean, P., Heilmann, C., Weihe, P., Nielsen, F., Mogensen, U.B., Budtz-Jorgensen, E.,
589 2017. Serum Vaccine Antibody Concentrations in Adolescents Exposed to Perfluorinated
590 Compounds. Environ Health Persp 125.

591 Han, X., Nabb, D.L., Russell, M.H., Kennedy, G.L., Rickard, R.W., 2012. Renal Elimination of
592 Perfluorocarboxylates (PFCAs). Chemical Research in Toxicology 25, 35-46.

593 Harada, K., Inoue, K., Morikawa, A., Yoshinaga, T., Saito, N., Koizumi, A., 2005. Renal
594 clearance of perfluorooctane sulfonate and perfluorooctanoate in humans and their species-
595 specific excretion. Environmental Research 99, 253-261.

596 Hsueh, C.H., Yoshida, K., Zhao, P., Meyer, T.W., Zhang, L., Huang, S.M., Giacomini, K.M.,
597 2016. Identification and Quantitative Assessment of Uremic Solutes as Inhibitors of Renal
598 Organic Anion Transporters, OAT1 and OAT3. Mol Pharm 13, 3130-3140.

599 International Transporter Consortium, Giacomini, K.M., Huang, S.M., Tweedie, D.J., Benet, L.Z.,
600 Brouwer, K.L., Chu, X., Dahlin, A., Evers, R., Fischer, V., Hillgren, K.M., Hoffmaster, K.A.,
601 Ishikawa, T., Keppler, D., Kim, R.B., Lee, C.A., Niemi, M., Polli, J.W., Sugiyama, Y., Swaan,
602 P.W., Ware, J.A., Wright, S.H., Yee, S.W., Zamek-Gliszczynski, M.J., Zhang, L., 2010.
603 Membrane transporters in drug development. Nat Rev Drug Discov 9, 215-236.

604 Inui, K., Masuda, S., Saito, H., 2000. Cellular and molecular aspects of drug transport in the
605 kidney. Kidney Int 58, 944-958.

606 Kato, K., Wong, L.Y., Jia, L.T., Kuklenyik, Z., Calafat, A.M., 2011. Trends in Exposure to
607 Polyfluoroalkyl Chemicals in the US Population: 1999-2008. Environmental Science &
608 Technology 45, 8037-8045.

Kimoto, E., Mathialagan, S., Tylaska, L., Niosi, M., Lin, J., Carlo, A.A., Tess, D.A., Varma, M.V.S., 2018. Organic Anion Transporter 2-Mediated Hepatic Uptake Contributes to the Clearance of High-Permeability-Low-Molecular-Weight Acid and Zwitterion Drugs: Evaluation Using 25 Drugs. Journal of Pharmacology and Experimental Therapeutics 367, 322-334.

Kudo, N., Suzuki, E., Katakura, M., Ohmori, K., Noshiro, R., Kawashima, Y., 2001. Comparison of the elimination between perfluorinated fatty acids with different carbon chain length in rats. Chem-Biol Interact 134, 203-216.

Lau, C., Anitole, K., Hodes, C., Lai, D., Pfahles-Hutchens, A., Seed, J., 2007. Perfluoroalkyl acids: A review of monitoring and toxicological findings. Toxicological Sciences 99, 366-394.

Launay-Vacher, V., Izzedine, H., Karie, S., Hulot, J.S., Baumelou, A., Deray, G., 2006. Renal tubular drug transporters. Nephron Physiol 103, 97-106.

Lepist, E.I., Zhang, X.X., Hao, J., Huang, J., Kosaka, A., Birkus, G., Murray, B.P., Bannister, R., Cihlar, T., Huang, Y., Ray, A.S., 2014. Contribution of the organic anion transporter OAT2 to the renal active tubular secretion of creatinine and mechanism for serum creatinine elevations caused by cobicistat. Kidney Int 86, 350-357.

Lin, J.Y., Chin, S.Y., Tan, S.P.F., Koh, H.C., Cheong, E.J.Y., Chan, E.C.Y., Chan, J.C.Y., 2023. Mechanistic Middle-Out Physiologically Based Toxicokinetic Modeling of Transporter-Dependent Disposition of Perfluorooctanoic Acid in Humans. Environmental Science & Technology 57, 6825-6834.

Lin, P.I.D., Cardenas, A., Hauser, R., Gold, D.R., Kleinman, K.P., Hivert, M.F., Fleisch, A.F., Calafat, A.M., Webster, T.F., Horton, E.S., Oken, E., 2019. Per- and polyfluoroalkyl substances and blood lipid levels in pre-diabetic adults-longitudinal analysis of the diabetes prevention program outcomes study. Environ Int 129, 343-353.

Louisse, J., Dellafiora, L., van den Heuvel, J.J.M.W., Rijkers, D., Leenders, L., Dorne, J.-L.C.M., Punt, A., Russel, F.G.M., Koenderink, J.B., 2023. Perfluoroalkyl substances (PFASs) are substrates of the renal human organic anion transporter 4 (OAT4). Archives of Toxicology 97, 685-696.

Lucas, K., Gaines, L.G.T., Paris-Davila, T., Nylander-French, L.A., 2023. Occupational exposure and serum levels of per- and polyfluoroalkyl substances (PFAS): A review. Am J Ind Med 66, 379-392.

Martinez, B., Da Silva, B.F., Aristizabal-Henao, J.J., Denslow, N.D., Osborne, T.Z., Morrison, E.S., Bianchi, T.S., Bowden, J.A., 2022. Increased levels of perfluorooctanesulfonic acid (PFOS) during Hurricane Dorian on the east coast of Florida. Environ Res 208, 112635.

Masereeuw, R., Russel, F.G.M., 2001. Mechanisms and clinical implications of renal drug excretion. Drug Metab Rev 33, 299-351.

Masungi, C., Mensch, J., Van Dijck, A., Borremans, C., Willems, B., Mackie, C., Noppe, M., Brewster, M.E., 2008. Parallel artificial membrane permeability assay (PAMPA) combined with a 10-day multiscreen Caco-2 cell culture as a tool for assessing new drug candidates. Pharmazie 63, 194-199.

Mathialagan, S., Bi, Y.A., Costales, C., Kalgutkar, A.S., Rodrigues, A.D., Varma, M.V.S., 2020. Nicotinic acid transport into human liver involves organic anion transporter 2 (SLC22A7). Biochem Pharmacol 174.

Mathialagan, S., Piotrowski, M.A., Tess, D.A., Feng, B., Litchfield, J., Varma, M.V., 2017. Quantitative Prediction of Human Renal Clearance and Drug-Drug Interactions of Organic Anion Transporter Substrates Using In Vitro Transport Data: A Relative Activity Factor Approach. Drug Metabolism and Disposition 45, 409-417.

Nakagawa, H., Hirata, T., Terada, T., Jutabha, P., Miura, D., Harada, K.H., Inoue, K., Anzai, N., Endou, H., Inui, K.I., Kanai, Y., Koizumi, A., 2008. Roles of organic anion transporters in the renal excretion of perfluorooctanoic acid. Basic Clin Pharmacol 103, 1-8.

Nakagawa, H., Terada, T., Harada, K.H., Hitomi, T., Inoue, K., Inui, K., Koizumi, A., 2009. Human Organic Anion Transporter hOAT4 is a Transporter of Perfluorooctanoic Acid. Basic Clin Pharmacol 105, 136-138.

Nigam, S.K., Bush, K.T., Martovetsky, G., Ahn, S.Y., Liu, H.C., Richard, E., Bhatnagar, V., Wu, W., 2015. The Organic Anion Transporter (Oat) Family: A Systems Biology Perspective. Physiol Rev 95, 83-123.

Niu, S., Cao, Y.X., Chen, R.W., Bedi, M., Sanders, A.P., Ducatman, A., Ng, C., 2023. A State-of-the-Science Review of Interactions of Per- and Polyfluoroalkyl Substances (PFAS) with Renal Transporters in Health and Disease: Implications for Population Variability in PFAS Toxicokinetics. Environ Health Persp 131.

Nystrom, J., Benskin, J.P., Plassmann, M., Sandblom, O., Glynn, A., Lampa, E., Gyllenhammar, I., Moraeus, L., Lignell, S., 2022. Demographic, life-style and physiological determinants of serum per- and polyfluoroalkyl substance (PFAS) concentrations in a national cross-sectional survey of Swedish adolescents. Environ Res 208, 112674.

Ohmori, K., Kudo, N., Katayama, K., Kawashima, Y., 2003. Comparison of the toxicokinetics between perfluorocarboxylic acids with different carbon chain length. Toxicology 184, 135-140.

Oja, M., Sild, S., Maran, U., 2019. Logistic Classification Models for pH-Permeability Profile: Predicting Permeability Classes for the Biopharmaceutical Classification System. J Chem Inf Model 59, 2442-2455.

677 Olsen, G.W., Burris, J.M., Ehresman, D.J., Froehlich, J.W., Seacat, A.M., Butenhoff, J.L., Zobel,
678 L.R., 2007. Half-life of serum elimination of perfluorooctanesulfonate, perfluorohexanesulfonate,
679 and perfluorooctanoate in retired fluorochemical production workers. Environ Health Persp 115,
680 1298-1305.

681 Olsen, G.W., Mair, D.C., Lange, C.C., Harrington, L.M., Church, T.R., Goldberg, C.L., Herron,
682 R.M., Hanna, H., Nobiletti, J.B., Rios, J.A., Reagen, W.K., Ley, C.A., 2017. Per- and
683 polyfluoroalkyl substances (PFAS) in American Red Cross adult blood donors, 2000-2015.
684 Environmental Research 157, 87-95.

685 Pizzurro, D.M., Seeley, M., Kerper, L.E., Beck, B.D., 2019. Interspecies differences in
686 perfluoroalkyl substances (PFAS) toxicokinetics and application to health-based criteria. Regul
687 Toxicol Pharm 106, 239-250.

688 Ryu, S., Woody, N., Chang, G., Mathialagan, S., Varma, M.V.S., 2022. Identification of Organic
689 Anion Transporter 2 Inhibitors: Screening, Structure-Based Analysis, and Clinical Drug
690 Interaction Risk Assessment. J Med Chem 65, 14578-14588.

691 Shen, H., Lai, Y.R., Rodrigues, A.D., 2017. Organic Anion Transporter 2: An Enigmatic Human
692 Solute Carrier. Drug Metabolism and Disposition 45, 228-236.

693 Shima, J.E., Komori, T., Taylor, T.R., Stryke, D., Kawamoto, M., Johns, S.J., Carlson, E.J.,
694 Ferrin, T.E., Giacomini, K.M., 2010. Genetic variants of human organic anion transporter 4
695 demonstrate altered transport of endogenous substrates. Am J Physiol Renal Physiol 299,
696 F767-775.

697 Sun, H., Frassetto, L., Benet, L.Z., 2006. Effects of renal failure on drug transport and
698 metabolism. Pharmacol Therapeut 109, 1-11.

699 Thompson, J., Roach, A., Eaglesham, G., Bartkow, M.E., Edge, K., Mueller, J.F., 2011.
700 Perfluorinated alkyl acids in water, sediment and wildlife from Sydney Harbour and
701 surroundings. Mar Pollut Bull 62, 2869-2875.

702 Tucker, G.T., 1981. Measurement of the Renal Clearance of Drugs. Brit J Clin Pharmaco 12,
703 761-770.

704 Ullrich, K.J., 1997. Renal transporters for organic anions and organic cations. Structural
705 requirements for substrates. J Membrane Biol 158, 95-107.

706 Vandenheuvel, J.P., Kuslikis, B.I., Vanrafelghem, M.J., Peterson, R.E., 1991. Tissue
707 Distribution, Metabolism, and Elimination of Perfluorooctanoic Acid in Male and Female Rats. J
708 Biochem Toxicol 6, 83-92.

709 Varma, M.V., Gardner, I., Steyn, S.J., Nkansah, P., Rotter, C.J., Whitney-Pickett, C., Zhang, H.,
710 Di, L., Cram, M., Fenner, K.S., El-Kattan, A.F., 2012a. pH-Dependent solubility and permeability
711 criteria for provisional biopharmaceutics classification (BCS and BDDCS) in early drug
712 discovery. Mol Pharm 9, 1199-1212.

713 Varma, M.V., Steyn, S.J., Allerton, C., El-Kattan, A.F., 2015. Predicting Clearance Mechanism
714 in Drug Discovery: Extended Clearance Classification System (ECCS). Pharmaceutical
715 Research 32, 3785-3802.

716 Varma, M.V.S., Chang, G., Lai, Y.R., Feng, B., El-Kattan, A.F., Litchfield, J., Goosen, T.C.,
717 2012b. Physicochemical Property Space of Hepatobiliary Transport and Computational Models
718 for Predicting Rat Biliary Excretion. Drug Metabolism and Disposition 40, 1527-1537.

719 Varma, M.V.S., Feng, B., Obach, R.S., Troutman, M.D., Chupka, J., Miller, H.R., El-Kattan, A.,
720 2009. Physicochemical Determinants of Human Renal Clearance. Journal of Medicinal
721 Chemistry 52, 4844-4852.

722 Wang, Z., DeWitt, J.C., Higgins, C.P., Cousins, I.T., 2017. A Never-Ending Story of Per- and
723 Polyfluoroalkyl Substances (PFASs)? Environ Sci Technol 51, 2508-2518.

724 Weaver, Y.M., Ehresman, D.J., Butenhoff, J.L., Hagenbuch, B., 2010. Roles of rat renal organic
725 anion transporters in transporting perfluorinated carboxylates with different chain lengths.
726 Toxicol Sci 113, 305-314.

727 Worley, R.R., Fisher, J., 2015. Application of physiologically-based pharmacokinetic modeling to
728 explore the role of kidney transporters in renal reabsorption of perfluorooctanoic acid in the rat.
729 Toxicol Appl Pharm 289, 428-441.

730 Yang, C.H., Glover, K.P., Han, X., 2010. Characterization of Cellular Uptake of
731 Perfluorooctanoate via Organic Anion-Transporting Polypeptide 1A2, Organic Anion Transporter
732 4, and Urate Transporter 1 for Their Potential Roles in Mediating Human Renal Reabsorption of
733 Perfluorocarboxylates. Toxicological Sciences 117, 294-302.

734 Zhang, S., Lovejoy, K.S., Shima, J.E., Lagpacan, L.L., Shu, Y., Lapuk, A., Chen, Y., Komori, T.,
735 Gray, J.W., Chen, X., Lippard, S.J., Giacomini, K.M., 2006. Organic cation transporters are
736 determinants of oxaliplatin cytotoxicity. Cancer Res 66, 8847-8857.

737 Zhang, Y., Beesoon, S., Zhu, L., Martin, J.W., 2013. Biomonitoring of perfluoroalkyl acids in
738 human urine and estimates of biological half-life. Environ Sci Technol 47, 10619-10627.

739